NATIONAL RADIO ASTRONOMY OBSERVATORY
SOCORRO, NEW MEXICO
VERY LARGE ARRAY PROGRAM

VLA ELECTRONICS MEMORANDUM NO. 183

HARMFUL INTERFERENCE LEVELS FOR THE VLA

A. R. Thompson

July 1979

1.0 INTRODUCTION

This memorandum describes an estimate of the threshold levels of harmful interference for observations with the VLA.[1] The conditions considered are the standard mapping mode of operation in which a point in the sky is tracked over an hour-angle range of -4 to +4 hours, and a source of interference that is stationary relative to the array. It is assumed that the interference is received in the far side-lobes of the antennas where the gain is equal to that of an isotropic radiator. The study is aimed, in particular, at the effects of the proposed Satellite Power System which would require satellites in geosynchronous equatorial orbits. Preliminary results of the present study were reported at the Battelle Institute Workshop on the effects of the SPS on astronomy, held in Seattle, Washington, May 23-24, 1979.

Harmful interference levels for radio astronomy observations in general are given in CCIR Report 224-4. These levels were derived for measurements of the total power received by a single large antenna, which is the type of radio astronomy observation most vulnerable to interference. For an array of spaced antennas, working in the Fourier Synthesis mode, two effects help to discriminate against signals emanating from sources other than that under observation. As a result, levels of interference somewhat higher than those of CCIR 224-4 may be tolerable. The CCIR levels, of course, remain the general criterion, since arrays are not suited to all types of observations and single antennas will continue to be widely used.

In the VLA, 27 antennas are arranged in a Y-shaped configuration

---

[1] Supersedes earlier calculations in VLA Electronics Memorandum No. 129.

with arms 21 km long (Heeschen 1975). The outputs from the individual antennas are combined in pairs to provide the time-averaged signal products from which the complex fringe visibility V(u,v) can be derived. The quantities u and v are the components of the antenna spacing measured in wavelengths in a plane normal to the direction of observation, and towards the east and north respectively. V(u,v) is the Fourier Transform of B(x,y), the two-dimensional brightness distribution on the sky, where x and y are measured in radians towards the east and north respectively. At any given instant, each antenna-pair provides data at one point in the (u,v) plane, and as the earth rotates and the antennas track the point under observation across the sky, the corresponding point in the (u,v) plane traces out a portion of an elliptical locus. The placement of the antennas in the array is designed to optimize the sampling in the (u,v) plane by the 351 ellipses generated by the 27 antennas. This optimization covers observing declinations from -20° to the north pole with a tracking range of -4 hours to +4 hours about the meridian. After an observation has been made the recorded visibility data are interpolated to provide values at points on a rectangular grid in the (u,v) plane, and Fourier Transformation then produces a grid of points representing B(x,y).

The first of the effects that reduce the response to unwanted signals is the sidereal motion of cosmic sources across the sky, which results in changes in the relative phases of the signals at the antennas. This effect can be described as the motion of the source through the fringe pattern of each pair of antennas, and in a simple interferometer system it causes the output of the signal multiplier to vary quasi-sinusoidally[1] with time at a frequency referred to as the natural fringe frequency. In the VLA compensating phase changes are introduced into the local oscillator system so that

[1]The output waveform has a frequency that varies slowly with time but over any short period closely resembles a sine wave.

the phase of the signals from a point source remains constant at the multiplier outputs.[1] With this scheme, signals from a stationary source produce multiplier outputs at the natural fringe rate corresponding to the point under observation. The interpolation process that precedes Fourier Transformation involves time averaging, and any sinusoidally varying components are thereby reduced. The second reduction effect applies only to broadband signals. In order to preserve the correlation of the cosmic signals it is necessary to insert variable time delays in the signal paths to compensate for the differences in the transmission paths from the source under observation to the individual antennas. The time delays for a signal from an interfering source are generally not equal so broadband interfering signals are to some extent decorrelated.

Both of the effects depend in a complicated manner upon the configuration of the antennas in the array and the celestial coordinates of the point under observation. A precise general expression for the overall interference reduction is not obtainable, although numerical solutions for particular cases can, of course, be derived. The present approach is, when possible, to make approximations in order to derive simplified expressions which show the dependence on various parameters. Numerical solutions are used to support and extend such analysis.

2.0 FRINGE-FREQUENCY AVERAGING

Consider first the effect of averaging on the sinusoidal frequency components. The normal procedure for interpolating visibility data for the VLA is to divide the (u,v) plane into a series of rectangular cells of dimensions Δu by Δv, and to assign to the center point of each cell a visibility equal to the mean of all values falling within it. The quantities Δu and Δv are equal to the reciprocals of the dimensions of the field in the (x,y) plane to be mapped, and usually Δu and Δv are made equal. To determine the effects of averaging on the interfering signal at any point in the (u,v) plane it is necessary to know the

[1] To derive the phase of the visibility function two multipliers are used for each pair of signals, one having a quadrature phase shifter at one input.

product of the frequency of the sinusoidal variations at the multiplier output and the time taken for the locus of an antenna-pair to cross a cell.

The expressions for u and v are as follows:

$$\left.\begin{aligned} u &= B_x \sin H - B_y \cos H \\ v &= B_z \cos \delta - B_x \sin \delta \cos H - B_y \sin \delta \sin H \end{aligned}\right\} \qquad (1)$$

where H and δ are the hour angle and declination of the point under observation and B_x, B_y and B_z are components of the spacing between the two antennas measured in wavelengths in the directions ($H = 0^o$ $\delta = 0^o$), ($H = +90^o$ $\delta = 0^o$) and ($\delta = +90^o$) respectively.[1] For the present discussion it is convenient to consider also a (u',v') plane where $u' = u$ and $v' = v$ cosec δ. In the (u',v') plane the elliptical loci of the (u,v) plane become circles of radius $q' = (B_x^2 + B_y^2)^{\frac{1}{2}}$, each generated by a radius vector that rotates with a constant angular velocity ω_o equal to the rotation velocity of the earth. The centers of the circles are on the v' axis at $v' = B_z \cot \delta$. The cells in the (u',v') plane are rectangular, with dimensions Δu by $\Delta v|\text{cosec } \delta|$.

Figure 1 shows the locus for an antenna-pair crossing a cell at a point where the radius vector makes an angle ϕ with the v' axis. For simplicity, the path length through a cell is considered to be a straight line. Since the number of cells usually lies between 128 x 128 and 2048 x 2048, the fraction of the plane for which this assumption is inaccurate is relatively small. The path length through a cell will vary depending on whether the locus passes near the center of the cell or merely cuts across a corner. However, for cells in the vicinity of the point defined by the radius vector, the average cell-crossing length is approximately equal to the cell area, $\Delta u \Delta v$, divided by the projected cell width in the q' direction which is $\Delta u' \sin\phi + \Delta v' \cos\phi = \Delta u(\sin\phi + \text{cosec } \delta \cos \phi)$. Note that the expression is valid only for positive values of the trigonometric functions. The mean time to cross a cell is equal to

---

[1] As defined by Hogg et al. (1969) and used here. In the VLA software B_y is measured towards $H = -90^o$, $\delta = 0^o$.

$$\tau_\phi = \frac{\Delta u\,|\mathrm{cosec}\delta|}{\omega_o\, q'\,(|\sin\phi| + |\cos\phi|\,|\mathrm{cosec}\delta|)} \qquad (2)$$

The natural fringe frequency, f, for a source at (H,δ) is ω_o u cos δ, so the product $\tau_\phi f$ is

$$\tau_\phi f = \frac{\Delta u \sin\phi\,|\mathrm{cosec}\delta|\cos\delta}{|\sin\phi| + |\cos\phi|\,|\mathrm{cosec}\delta|} \qquad (3)$$

Note that $\tau_\phi f$ is independent of q' since both the fringe frequency and the cell-crossing speed are proportional to q'. Along the v' axis the fringe frequency goes to zero, and the averaging becomes ineffective. The fringe frequency also goes to zero for a source at the pole, $\delta = 90^o$.

An interfering signal of constant strength before the averaging is reduced in the averaging by a factor $\sin(\pi f\tau_\phi)/\pi f\tau_\phi$. The rms signal level integrated around the circular locus is thus proportional to a factor F_1 given by

$$F_1 = \left[\frac{2}{\pi}\int_o^{\pi/2}\left(\frac{|\sin\phi| + |\cos\phi|\,|\mathrm{cosec}\delta|}{\pi\Delta u \sin\phi\ \mathrm{cosec}\delta\ \cos\phi}\right)^2 \sin^2 \left(\frac{\pi\Delta u \sin\phi\ \mathrm{cosec}\delta\ \cos\delta}{|\sin\phi| + |\cos\phi|\,|\mathrm{cosec}\delta|}\right) d\phi\right]^{\frac{1}{2}} \qquad (4)$$

The above integral cannot be evaluated analytically without introducing some approximations. In practice Δu is unlikely to be less than 60 wavelengths; Δu^{-1} is the width of the synthesized field and 60 wavelengths is half the diameter of a VLA antenna at the longest presently-used wavelength of 21 cm. Commonly used values of Δu are 100 to a few thousand wavelengths. For $\Delta u = 60$ and $\phi = 10^o$ the sinc-squared function to be integrated in (4) has a value of about 10^{-3}. Thus most of the contribution to the integral occurs in the range $|\phi| < 10^o$ for which $\sin\phi \approx \phi$. Also in this range the mean path length through a cell is close to Δu, and using this constant value merely slightly underestimates the effect of averaging at larger values of ϕ. Finally the limit of integration can be extended from π to infinity without serious error.

The following expression should therefore provide an approximate estimate of F_1:

$$F_1 \simeq \left[\frac{2}{\pi}\int_0^{\infty} \frac{\sin^2(\pi\Delta u\phi\cos\delta)}{(\pi\Delta u\phi\ \cos\delta)^2}\, d\phi\right]^{\frac{1}{2}} \simeq \left[\frac{1}{\pi\Delta u\ \cos\delta}\right]^{\frac{1}{2}} \tag{5}$$

The next step is to derive the ratio of the sums of the squared amplitudes of the interference and the noise over the grid points in (u',v') plane. If S is the strength (flux density) of the interfering signal in W m^{-2}, and half the power is lost by polarization mismatch, the input signal power for an isotropic radiator is $S\lambda^2/8\pi$. After averaging, the sum of the squared signal amplitudes is proportional to

$$N\left[\frac{S\lambda^2 F_1}{8\pi}\right]^2 \tag{6}$$

where N is the number of (u,v) cells which contain data. The equivalent system noise level at the receiver inputs is $k\ T_s\ B$ where k is Boltzmann's constant, T_s is the system temperature and B is the receiving bandwidth. After averaging for a time τ_ϕ the rms noise level is reduced by a factor $[B\tau_\phi]^{-\frac{1}{2}}$. The sum of the squared noise amplitudes is, therefore,

$$\sum_N \frac{k^2 T_s^{\,2} B}{\tau_\phi} = k^2 T_s^{\,2} B \sum_N \tau_\phi^{-1} \tag{7}$$

where the sum is taken over the N sampled cells. To determine $\sum_N \tau_\phi^{-1}$, the mean of τ_ϕ^{-1} around a locus in the (u',v') plane is first derived:

$$\frac{2}{\pi}\int_0^{\pi/2} \tau_\phi^{-1} d\phi = \frac{2}{\pi}\int_0^{\pi/2} \frac{\omega_o\ q'\ (\sin\phi + |\mathrm{cosec}\delta|\ \cos\phi)\ d\phi}{\Delta u\ |\mathrm{cosec}\delta|}$$

$$= \frac{2\ \omega_o\ q'}{\pi\Delta u}\left[1 + |\sin\delta|\right] \tag{8}$$

Thus

$$\sum_N \tau_\phi^{-1} = \frac{2\omega_o}{\pi\Delta u} [1 + |\sin\delta|] \sum_N q' \qquad (9)$$

By Parseval's theorem (see, for example, Bracewell 1965) the ratio of the sum of the squared amplitudes of the signal and noise components in the (u,v) plane is equal to the corresponding ratio in the brightness distribution, B(x,y). Thus the ratio, R, of the rms levels of the signal and noise in B(x,y) is given by

$$R = \frac{S\lambda^2 F_1 \sqrt{\Delta u}}{8\sqrt{2\pi}\, k\, T_s \sqrt{B\omega_o (1 + |\sin\delta|)}} \left[\frac{1}{N}\sum_N q'\right]^{-\frac{1}{2}} \qquad (10)$$

If one inserts for R the maximum value for which the interference is a tolerably small fraction of the noise, the resulting value of S represents the harmful threshold of the interfering signal:

$$S = \frac{8\sqrt{2}\, \pi\, R\, k\, T_s \sqrt{B\, \omega_o\, \cos\delta (1 + |\sin\delta|)}}{\lambda^2} \left[\frac{1}{N}\sum_N q'\right]^{\frac{1}{2}} \qquad (11)$$

where F_1 has been substituted for from equation (5). The dependence of S upon wavelength results from the effective collecting area of the antennas in the distant side-lobes. The dependence on bandwidth results from the terms for the magnitude of the noise power and the averaging factor for the noise. The factor cos δ results from the fringe-frequency dependence in the averaging of the signal. At $\delta = 90^\circ$ the fringe frequency becomes zero and the averaging factor in expression (4) becomes equal to unity. However, the approximation in expression (5) approaches infinity as δ approaches 90°. Thus equation (11) does not hold for declinations close to the pole, but this is not serious since a relatively small area of sky is involved.

Figure 2 is a plot of $[\cos\delta\ (1 + |\sin\delta|)]^{\frac{1}{2}}$ which shows that a constant value of 1.0 for this quantity is a fair approximation for all declinations except those close to the pole. The factor $(\frac{1}{N}\sum_N q')$

is the mean value of $\sqrt{B_x^2 + B_y^2}$, measured in wavelengths, over the cells of the (u,v) plane. Since the number of cells that any locus intersects is approximately proportional to q', the average of the 351 q' values, weighted in proportion to q', is required:

$$\frac{1}{N}\sum_{N} q' \simeq \sum_{351} q'^2 / \sum_{351} q' \qquad (12)$$

where $\sum_{351}$ represents the sum over the 351 baselines. The antennas of the VLA can be moved between four sets of foundations by means of a rail-mounted transporter, to vary the scale of antenna spacings in four steps, usually referred to as configurations A, B, C, and D. For simplicity only the largest (A) and the most compact (D) configurations will be considered here. For the A configuration equation (12) has an equivalent value in metres of 1.55×10^4 m and for the D configuration 436 m.

Finally, to determine the harmful interference thresholds it is necessary to assign a value to R, the maximum tolerable ratio of interference to noise. The uncertainty here lies in how the interfering signal is likely to be distributed over B(x,y). If it produces a generally-uniform, randomly-varying component similar to the noise, a value of 10^{-1} for R should be acceptable. If, on the other hand, the interference components combine to form isolated peaks the effect would be more serious, and a lower value of R would be necessary. It is to be expected that from one antenna-pair to another the interference will be largely random in phase, since the far side-lobe patterns of the antennas are unlikely to be identical. For a single antenna-pair the averaged phase will show progressive shifts from cell to cell of the (u,v) plane, and so will not vary randomly along a locus. However, if the cell size is large, two or more loci may often traverse a cell, and this effect will tend to further randomize the phases. The concentration of the high amplitude values of the averaged interference near the v axis of the (u,v) plane

should result in the interference component in the sky map, B(x,y) showing elongated structure the east-west direction. This effect has not been demonstrated since no observation has been made with the VLA in which an interfering signal was present at a constant level all of the time. Without further investigation one can do little more than guess that $R = 10^{-2}$ should be a safe criterion, and this value will now be used.

With the parameter values discussed above, equation (11) becomes

$$S = \begin{Bmatrix} 5{\cdot}20 \times 10^{-24} \text{ (config. A)} \\ 8{\cdot}73 \times 10^{-25} \text{ (config. D)} \end{Bmatrix} \frac{T_s B^{\frac{1}{2}}}{\lambda^{5/2}} \text{ W m}^{-2} \qquad (13)$$

where T_s is measured in Kelvins, B in Hz and λ in m. Values of S are given in Table I for the four wavelength bands of the VLA and configurations A and D.

To examine the effect of the approximations introduced in using the simplified expression for F_1 in equation (5), the following expression was evaluated by computation:

$$F_1 = \left[\sum \frac{q' \sin^2(\pi \tau_\phi f)}{(\pi \tau_\phi f)^2} \Big/ \sum q' \right]^{\frac{1}{2}} \qquad (14)$$

Values of u', ϕ and $\tau_\phi f$ were determined for each of the 351 baselines for 30-second intervals in hour angle from -4 to +4 hours. The summation in equation (14) was taken over the resulting points, and the weighting factor q' helps to compensate for the uneven distribution in the (u,v) plane of points resulting from incremental sampling in hour angle. For declination $\delta = 30^\circ$, Table I includes a comparison of values of F_1 determined from equations (5) and (14). The results agree within 1.4 dB, the values from equation (5) being slightly higher. In Figure 3 the results are compared as a function of declination for the D configuration at 6-cm wavelength. It can be concluded that equation (5) provides a satisfactory approximation for the effect of fringe-frequency averaging. Note that although F_1 depends upon Δu, which is determined by

the size of the synthesized field, S is independent of Δu because the averaging of the noise and the interference depend upon Δu in a similar manner.

The effect of fringe-frequency averaging will depend to some extent on the method of data reduction used, and the above results have been derived for the common practice of cell averaging followed by discrete Fourier transformation. The use of a different interpolating function, such as a Gaussian, has not been investigated. The averaging in the (u,v)-plane could be avoided by direct Fourier transformation, but the combination of the data in the transformation process should have an effect similar to that of averaging. In fact, the cutoff of the brightness function at some finite dimensions can be regarded as equivalent to a convolution in the (u,v)-plane. Since the width of the convolving function is inversely proportional to the width of the synthesized field, one might expect that the interference in the map should show an increase in amplitude from the center to the edges.

3.0 DECORRELATION OF BROADBAND SIGNALS

The decorrelation of a broadband interfering signal by inequality in the time delays of the signal paths can significantly reduce the unwanted response. However the magnitude of the reduction is, for several reasons, less easy to calculate than for the fringe-frequency averaging effect. First, the delay required to compensate for the signals from the point being observed is not uniquely defined by the position in the (u,v) plane, but also depends upon the spacing and azimuth of the pair of antennas concerned. Second, it depends upon the position of the source of interference. Third, the decorrelation factor depends upon the uniformity of the power flux density across the signal spectrum. It will be assumed here that the signal has the characteristics of thermal noise, but if it includes narrowband components such as spurious oscillations from malfunctioning transmitter modules of a power satellite the reduction will not be as effective.

Consider a single baseline, the direction of which is defined by the hour angle h and declination d of the end nearest the north pole. If the direction of observation, (H,δ), makes an angle θ with the normal to the baseline, the difference in the space transmission paths to the two antennas is d sin θ. The angle θ is given by

$$\sin\theta = \sin\delta \sin d + \cos\delta \cos d \cos (H-h) \tag{15}$$

For any pair of antennas, lines of constant delay-difference on the celestial sphere are small circles concentric with the antenna baseline. As the antennas track, the instrumental delays are adjusted to equalize the paths for the required direction. The circle for which the delays are equalized thus moves across the sky as indicated in Figure 4, and, depending on several parameters, it may or may not sweep through the position of a satellite.

Consider a satellite in geosynchronous orbit, and suppose for simplicity that it is on the celestial meridian. The declination seen from the VLA Site will then be approximately $-5{\cdot}5^{\circ}$. The delay mismatch for signals from the satellite is

$$\tau = \ell(\sin\theta_1 - \sin\theta_2)/c \tag{16}$$

where ℓ is the length of the baseline, $(90^{\circ}-\theta_1)$ is the angle between the direction of the satellite and the baseline, and $(90^{\circ}-\theta_2)$ is the angle between the direction of observation and the baseline, and c is the velocity of light. If the receiving passband can be approximated by a rectangular function of width B, the delay mismatch produces a decrease in correction by a factor

$$\frac{\sin(\pi B\tau)}{\pi B\tau} \tag{17}$$

The half-amplitude points of the above function occur for $B\tau = \pm 0{\cdot}6$, and define a zone of high correlation which tracks the point being observed.

Now consider the width of the zone when it is centered on the position of the satellite, i.e., $\theta_1 = \theta_2$. The decorrelation factor will be greater than one-half for an angular range $\Delta\theta$ given by

$$\Delta\theta = \frac{1{\cdot}2}{B} \Big/ \frac{dT}{d\theta_2} = \frac{1{\cdot}2\ c}{B\ \ell\ \cos\theta_2} \qquad (18)$$

The solid angle of the zone on the hemisphere above the horizon is $\pi \sin\theta_2\ \Delta\theta$, and the fraction of the sky that it covers is

$$f = \frac{|\sin\theta_2\ \Delta\theta|}{2} = \frac{0{\cdot}6\ c\ |\tan\theta_2|}{B\ \ell} \qquad (19)$$

The value of $|\tan\theta_2|$ generally lies within the range 0 to 3, so one can expect that for roughly a fraction $c/B\ \ell$ of the time the signals from the satellite received by any antenna-pair will be very little decorrelated. At other times the decorrelation can be large.

The behavior of the decorrelation is similar to that of fringe-frequency averaging except that for the latter the function $\sin(\pi f\tau_\phi)/\pi f\tau_\phi$ peaks on the v axis of the (u,v)-plane whereas the decorrelation function $\sin(\pi BT)/\pi BT$ can peak at any point in the (u,v)-plane depending upon the azimuth of the baseline, the position of the interfering source, etc. Those baselines for which the two peaks happen to overlap will contribute very strongly to the interference in the data, and those for which the peaks are well separated in hour angle will contribute relatively little. In making a quantitative estimate of the effect of decorrelation it is therefore necessary to consider the two effects in combination. A factor F_2 was computed which is the rms of the product of the fringe averaging and decorrelation factors, divided by F_1:

$$F_2 = \left[\sum \frac{q'\ \sin^2(\pi f\tau_\phi)}{(\pi f\tau_\phi)^2}\ \frac{\sin^2(\pi BT)}{(\pi BT)^2} \Big/ \sum q'\right]^{\frac{1}{2}} \Big/ F_1 \text{ - - - - -} \qquad (20)$$

Thus F_2 gives the interference rejection resulting from decorrelation additional to that from fringe-frequency averaging. In computing F_2 the summation was taken over the 351 baselines at intervals of 2 minutes in hour angle from -4 to +4 hours as described for the computations in Section 2.0.

Some values for $\delta=30^{\circ}$ are given in Table I. The expected dependence on Δu should be noted: decreasing Δu increases the width of the function $\sin(\pi f\tau_\phi)/\pi f\tau_\phi$ and thus increases the overlap with maxima of $\sin(\pi BT)/\pi BT$. Decorrelation should therefore be least effective for the D array with the lowest values of Δu likely to be used, and this case is included in Table I.

Figure 5(a) shows the dependence of F_2 upon declination for a geosynchronous satellite on the meridian. The decorrelation is clearly most effective for observing declinations between 10° and 80°. The increase in F_2 near the pole results from the decrease in fringe-frequency in that region which causes the peak of the $\sin(\pi f\tau_\phi)/\pi f\tau_\phi$ function to broaden and thus overlap the peak in the decorrelation function for a greater number of baselines. The maximum value of F_2 occurs for an observing declination equal to that of the satellite. As the antennas track through the position of the satellite there is then no decorrelation of the interfering signal. Furthermore, for those baselines with azimuths close to 0° the fringe-frequency goes to zero at the same time: the spacial frequency vector in the (u,v)-plane crosses the v axis when the point under observation passes through the plane containing the baseline and the pole. Figure 4 illustrates the geometry involved. The nine antennas on the north arm of the VLA produce 36 approximately north-south baselines, so for 36 out of 351 baselines the decorrelation will have a small effect. Under these circumstances, decorrelation will reduce the mean squared interference response taken over all baselines by a factor of 10, and the rms response by $\sqrt{10}$, or 5 dB. This conclusion is in good agreement with the peaks in Figure 5(a) for configuration D. The curve for configuration A at 6 cm is lower for all declinations, which would be expected since the use of

the longer spacings result in narrower peaks for $\sin(\pi BT)/\pi BT$. From Figure 4 it can be seen that for declinations north of that of the satellite, and baselines close to north-south, the delays in the signal paths never become equal for signals from the satellite. For declinations south of that of the satellite they do become equal at some hour angle. Thus F_2 falls off more sharply to the north of $-5{\cdot}5^{\circ}$ than to the south.

Figure 5(b) shows the variation of F_2 for various satellite hour angles. The general behavior does not vary greatly, but subsidiary maxima appear, presumably related to the particular distribution of the baselines in azimuth. For the D configuration the overall magnitude of F_2 for observing declinations 20° to 80° and satellite hour angles 0° to 60° will be taken to be -17 dB for 50-MHz bandwidth and correspondingly -14 dB for 25-MHz bandwidth. The bandwidth dependence comes from the results in Table I.

4.0 CONCLUSION

To determine thresholds of harmful interference the results for configuration D should be used since they represent the worst case, in which the interference reduction is least effective. For narrowband interference, values are given in column 3 of Table II which were obtained by decreasing the value of S in Table I by 3 dB to make some allowance for the increase in F_1 at high declinations. These should be accurate for declinations from -20° to $+75^{\circ}$, and they apply to the receiving bandwidths shown in column 2 of Table II. Since $S \propto B^{\frac{1}{2}}$ in equation (11) the harmful levels for the narrowband case should be decreased if narrower bandwidths are considered.

The harmful levels for broadband signals, which are the ones of main interest with regard to the Satellite Power System, are obtained by dividing the narrowband levels in Table II by the receiving bandwidth to obtain values in W m^{-2} Hz^{-1}, and including the effect of decorrelation. The resulting power flux densities are proportional to $B^{-3/2}$ and the greatest sensitivity to interference thus occurs with the full bandwidths

shown. The use of F_2 = -17 dB for 50-MHz bandwidth and -14 dB for 25 MHz results in the harmful thresholds given in column 4 of Table II, which are appropriate for observing declinations from $+20^{\circ}$ to $+75^{\circ}$. The lowest values of harmful thresholds occur for an observing declination equal to that of the satellite, for which a value of about -4 dB is appropriate for F_2. The resulting harmful thresholds are given in column 5 of Table II and are equal to the values of S/B increased by 4 dB. Column 6 gives, for comparison, the corresponding broadband limits from CCIR Report 224-4. Column 7 gives the difference between the values in columns 4 and 6 which is the margin by which broadband interference can exceed the CCIR levels for the VLA for observations over much of the northern sky. Column 8 gives the equivalent margin at the declination of the satellite.

In the future the estimates derived here will probably be subject to some revision. In particular the use of $R = 10^{-2}$ is highly arbitrary, and experimental investigation to determine the distribution of the interfering component in a radio map should help define this criterion more precisely. Optional procedures in the data analysis, such as introduction of tapering of the visibility values in the (u,v) plane, influence the response to the interfering signals, and any values for tolerable levels should be regarded as guidelines rather than precisely defined quantities.

REFERENCES

CCIR Report 224-4, XIVth Plenary Assembly, Kyoto, 1978, published by International Telecommunications Union, Geneva, 1978.

TABLE I: FRINGE-FREQUENCY AVERAGING AND DECORRELATION EFFECTS

Wavelength, λ	21 cm		6 cm		2 cm		1·3 cm	
System Temp., T_s	50 K		50 K		50 K[1]		50 K[1]	
Bandwidth, B	25 MHz		50 MHz		50 MHz		50 MHz	
Configuration	A	D	A	D	A	D	A	D
S Wm^{-2}	$6{\cdot}4\times10^{-17}$	$1{\cdot}1\times10^{-17}$	$2{\cdot}1\times10^{-15}$	$3{\cdot}5\times10^{-16}$	$3{\cdot}2\times10^{-14}$	$5{\cdot}5\times10^{-15}$	$9{\cdot}5\times10^{-14}$	$1{\cdot}6\times10^{-14}$
S dB Wm^{-2}	-162	-170	-147	-155	-135	-143	-130	-137
Δu (Wavelengths)^2	300	60	1000	200	3000	600	5000	1000
F_1 (eqn. 5), $\delta=30^\circ$	$3{\cdot}50\times10^{-2}$	$7{\cdot}83\times10^{-2}$	1.92×10^{-2}	$4{\cdot}28\times10^{-2}$	$1{\cdot}11\times10^{-2}$	$2{\cdot}47\times10^{-2}$	$8{\cdot}57\times10^{-3}$	$1{\cdot}92\times10^{-2}$
F_1 (eqn. 13), $\delta=30^\circ$	$2{\cdot}57\times10^{-2}$	$5{\cdot}77\times10^{-2}$	$1{\cdot}47\times10^{-2}$	$3{\cdot}15\times10^{-2}$	$9{\cdot}84\times10^{-3}$	$1{\cdot}84\times10^{-2}$	$7{\cdot}59\times10^{-3}$	$1{\cdot}47\times10^{-2}$
S/B Wm^{-2} Hz^{-1}	$2{\cdot}6\times10^{-24}$	$4{\cdot}4\times10^{-25}$	$4{\cdot}2\times10^{-23}$	$7{\cdot}0\times10^{-24}$	$6{\cdot}4\times10^{-22}$	$1{\cdot}1\times10^{-22}$	$1{\cdot}9\times10^{-21}$	$3{\cdot}2\times10^{-22}$
S/B dB Wm^{-2} Hz^{-1}	-236	-244	-224	-232	-212	-220	-207	-215
F_2 dB, $\delta=30^\circ$	-31·8	-17·3	-35·0	-20·0	-35·7	-20·0	-36·2	-19·8

[1]Present system temperatures at 2 and 1·3 cm wavelength are approximately 250 K and 350 K respectively, but improvements in the near future should result in values close to 50 K.

TABLE II: HARMFUL THRESHOLDS FOR THE VLA COMPARED WITH HARMFUL LEVELS FROM CCIR REPORT 224-4

1 Wavelength Band	2 Receiving Bandwidth	3 Narrowband Harmful Level $\delta=-20^{\circ}$ to $+75^{\circ}$	4 Broadband Harmful Level $\delta=20^{\circ}$ to 75°	5 Broadband Harmful Level $\delta=-5.5^{\circ}$	6 CCIR 224-4 Harmful Level for Continuum	7 Margin Above CCIR 224-4 for $\delta=20^{\circ}$ to 75°	8 Margin Above CCIR 224-4 for $\delta=-5.5^{\circ}$
18-21 cm	25 MHz	-173 dB W m^{-2}	-233 dB W m^{-2} Hz^{-1}	-240 dB W m^{-2} Hz^{-1}	-255 dB W m^{-2} Hz^{-1}	22 dB	15 dB
6 cm	50 MHz	-158 dB W m^{-2}	-218 dB W m^{-2} Hz^{-1}	-228 dB W m^{-2} Hz^{-1}	-241 dB W m^{-2} Hz^{-1}	22 dB	13 dB
2 cm	50 MHz	-146 dB W m^{-2}	-206 dB W m^{-2} Hz^{-1}	-216 dB W m^{-2} Hz^{-1}	-233 dB W m^{-2} Hz^{-1}	27 dB	17 dB
1.3 cm	50 MHz	-140 dB W m^{-2}	-200 dB W m^{-2} Hz^{-1}	-210 dB W m^{-2} Hz^{-1}	-233 dB W m^{-2} Hz^{-1}	33 dB	23 dB

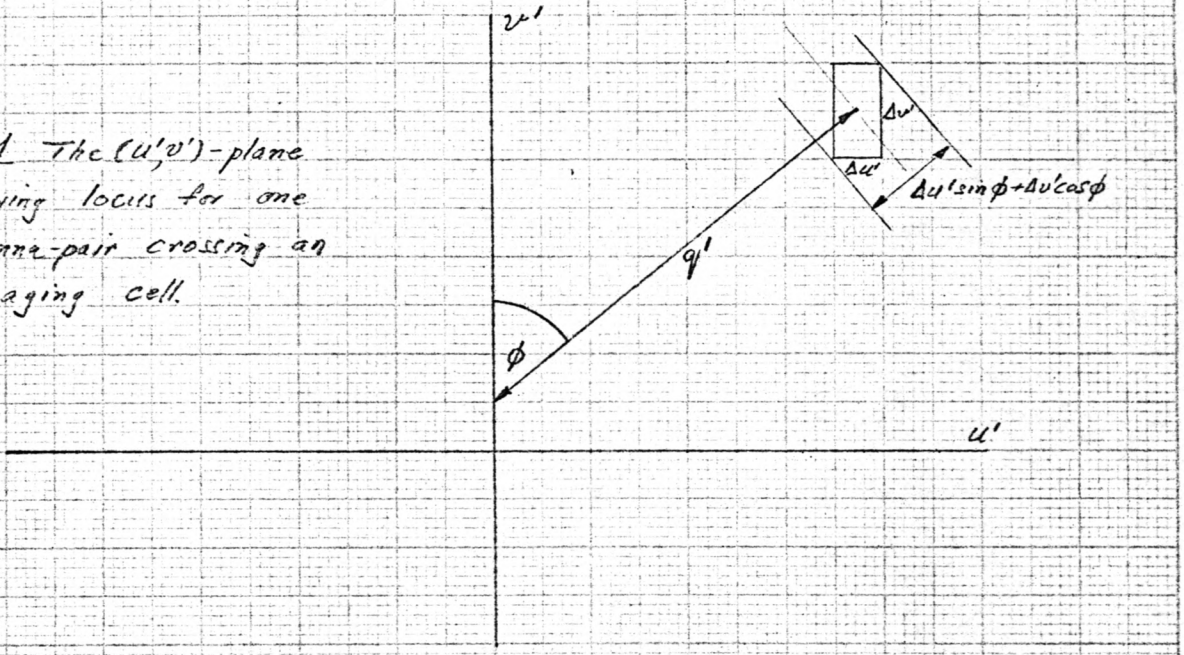

Fig. 1 The (u',v')-plane showing locus for one antenna-pair crossing an averaging cell.

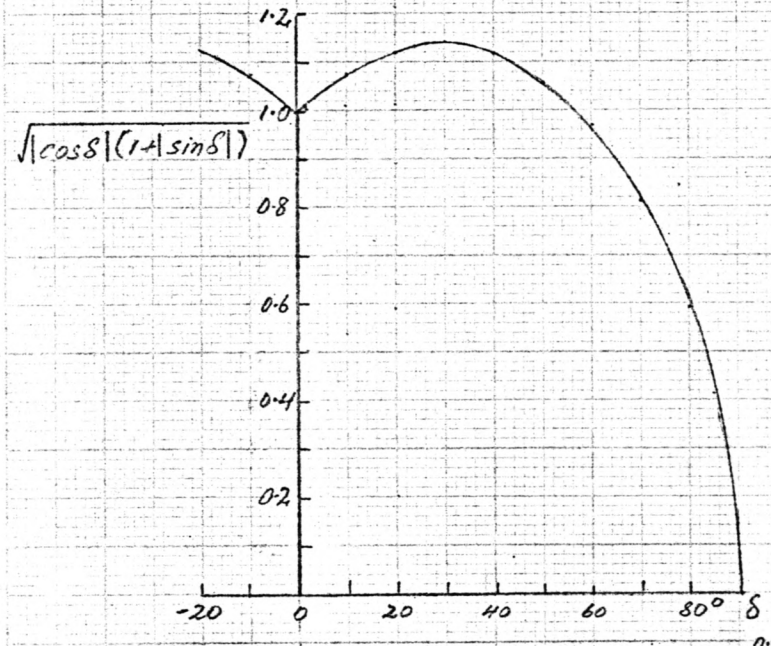

Fig 2 The function $\sqrt{|\cos\delta|(1+|\sin\delta|)}$. Use of a value 1.0 results in error < 2.2 dB in S for $-20° < \delta < 80°$.

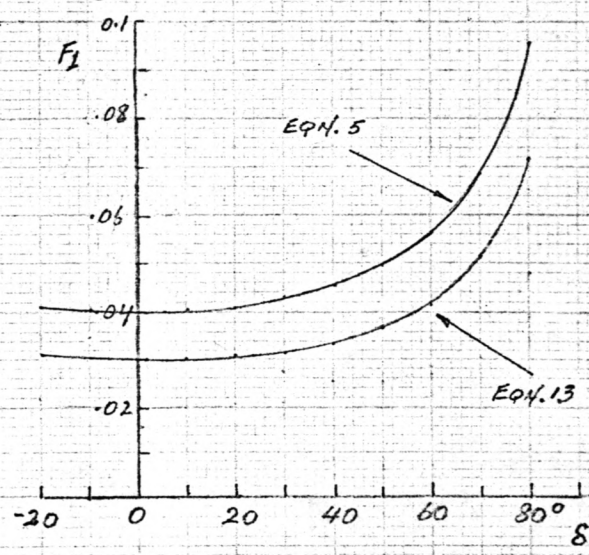

Fig 3 Comparison of values of F_1 as a function of δ, from equation 5 and from equation 13 (computed). Curves are for configuration D, 6 cm wavelength, and $\Delta u = 200$.

A.R.T. 5/12/79

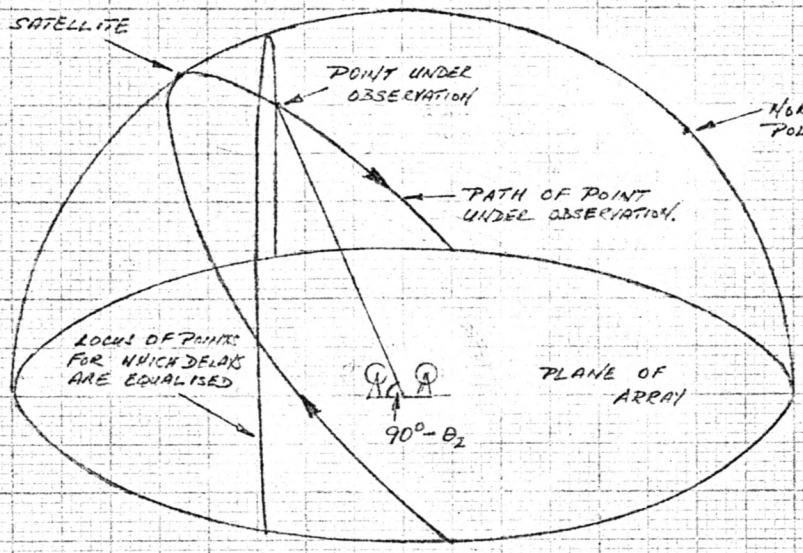

Fig. 4. Geometry of delay paths for one antenna-pair. Case shown is for N-S baseline and declination of observation equal to that of satellite.

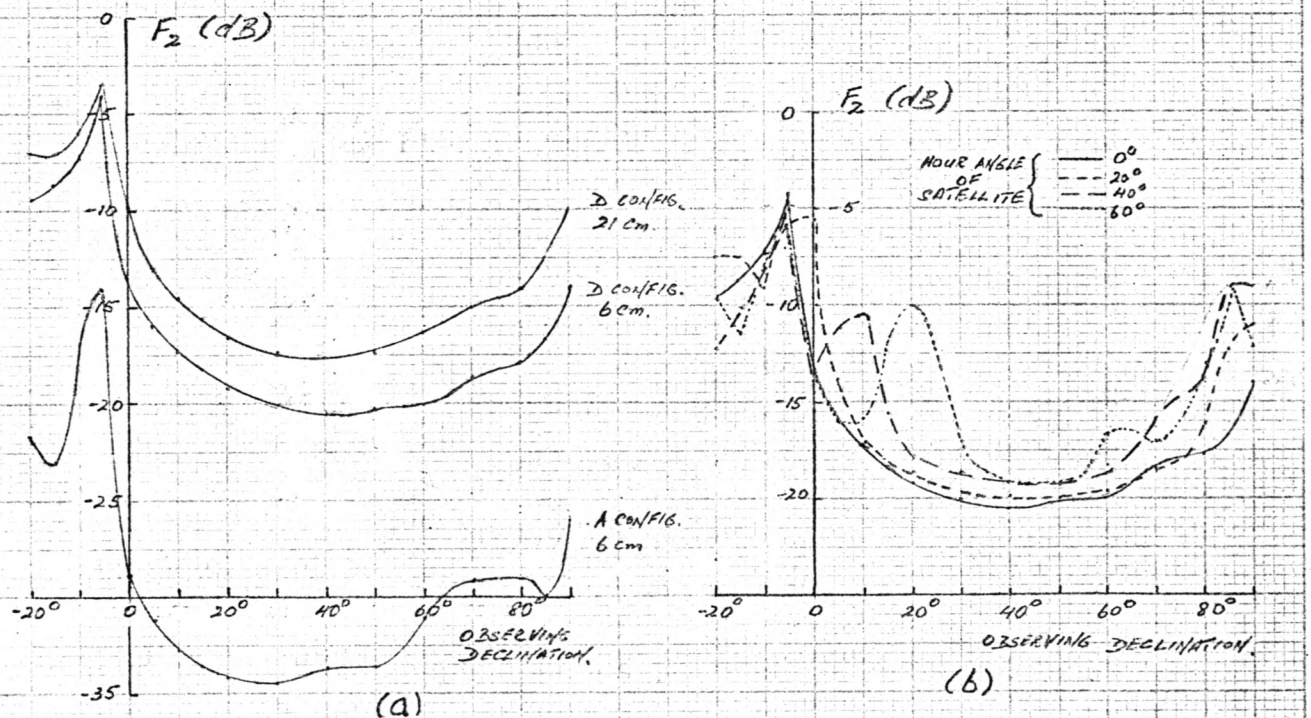

Fig 5. F_2, the reduction of broadband interference by decorrelation, plotted as a function of the declination of observation. (a) Curves for different configurations and wavelengths, all for satellite hour angle 0°. (b) Variation with satellite hour angle for configuration D at 6cm wavelength. Values of bandwidth and $\Delta\psi$ are those given in Table I.

A.R.T. 7/22/79